STUDY OF RECIPROCATING PUMP FOR SUPERCRITICAL ORC AT FULL AND PART LOAD OPERATION

Arnaud Landelle[1,2,3,4]*,Nicolas Tauveron[1,2],Philippe Haberschill[3],Rémi Revellin[3],Stephane Colasson[1,2]

[1] Université Grenoble Alpes, F-38000 Grenoble, France

[2] CEA, LITEN, LS2T, F-38000 Grenoble, France

[3] Université de Lyon, CNRS, INSA-Lyon, CETHIL, UMR5008, Villeurbanne F-69621, France

[4] ADEME, 20 Av. du Grésillé, BP90406, 49004 Angers Cedex 01, France

* arnaud.landelle@cea.fr

ABSTRACT

Recovery of waste heat in industrial processes is an important component of energy savings worldwide. At low temperature levels, thermodynamics prevents any high efficiency in the heat-to-electricity conversion; such dedicated systems have to be optimized and should achieve a maximum heat recovery, at partial and full load. These technical and technological problematic are also common with renewable natural resources use (solar, geothermal, biomass). Supercritical organic Rankine cycle is quite well investigated in the scientific community, but rarely experimentally studied, especially off-design and dynamic behaviors of such systems. The CEA/LITEN is developing a 10kWe prototypes of supercritical ORC to investigate experimental potential of such technology for low grade power generation. The first task is to characterize various components behavior in supercritical regimes. In such cycles, the pump plays a strategic role, as for supercritical operations the back work ratio is a key parameter to consider. Performance data of a reciprocating pump drive by an induction motor with variable speed drive are measured. Maximum pump efficiency achieve is 82% and maximum global efficiency (pump & drive) achieve is 41%. Losses are evaluated and a power model is proposed and compared with experimental data. Results of this work aim to give a better knowledge for ORC pump design and optimization.

1. INTRODUCTION

Organic Rankine Cycles (ORC) are known since the 19th century, but in recent decades research and commercial development increased exponentially (Quoilin *et al.*, 2013).Most research focused on nominal steady-state optimization, screening working fluid and operating conditions. Optimization criteria vary from study to study (energetic efficiency, exergetic analysis, power, or cost). Several study shows supercritical ORC have a high potential (Schuter *et al.*, 2010; Shu *et al.* 2013) especially in the low temperature range (~150°C) (Astolfi *et al.*, 2014; Toffolo *et al.*, 2014) but supercritical conditions mean high pressure and more constrains on components. For components optimization, most research focuses on the expander that is the critical components (Bao and Zhao, 2013), heat exchangers and evaporators especially are also investigated, but few researchers discuss of the pump. However, Quoilin *et al.* (2013) describes the pump as a key component that should be carefully chosen according to its controllability, tightness, Net Positive Suction Head (NPSH) and efficiency. Pump efficiency becomes a crucial parameter for low temperature and supercritical cycles. Back Work Ratio defines as the ratio between pump electrical consumption and expander outlet power is introduced to evaluate pump impact. In supercritical ORC, Maraver *et al.* (2014) shows that pump efficiency have a major impact on cycle exergetic efficiency. Using R-134a, cycle exergetic efficiency decrease from 46 to 40% if the pump efficiency decrease from 75 to 50 %. From authors' point of view, it is therefore essential to investigate the pumping system for on and off design ORC operation. The author listed only two pump efficiency correlation used for ORC models. A correlation is proposed by Lippke (1995) for centrifugal pump, losses related to the driver are also discussed. Quoilin *et al.* (2011) uses an empirical correlation proposed by Vetter (2006) for rotary positive displacement pump and add a constant electromechanical efficiency for driver losses. While most of feed pumps used in experimental ORC are reciprocating positive displacement pumps. Furthermore, as Miao *et al.* (2015) emphasized, confusions and simplifications are made about pump power consumption and efficiency. Results of this study aim to propose an experimental approach for pump characterization, a behavioural off-design reciprocating pump model for losses and efficiency that can be used for ORC system model, and provide knowledge assets for pump selection and optimal use.

2. EXPERIMENTAL SETUP

An experimental investigation is carried out on a diaphragm pump integrated into an experimental bench using R-134a as fluid. The test bench described in Figure 1 is use for subcritical and supercritical heat transfer investigation. This paper only focuses on the pumping system.

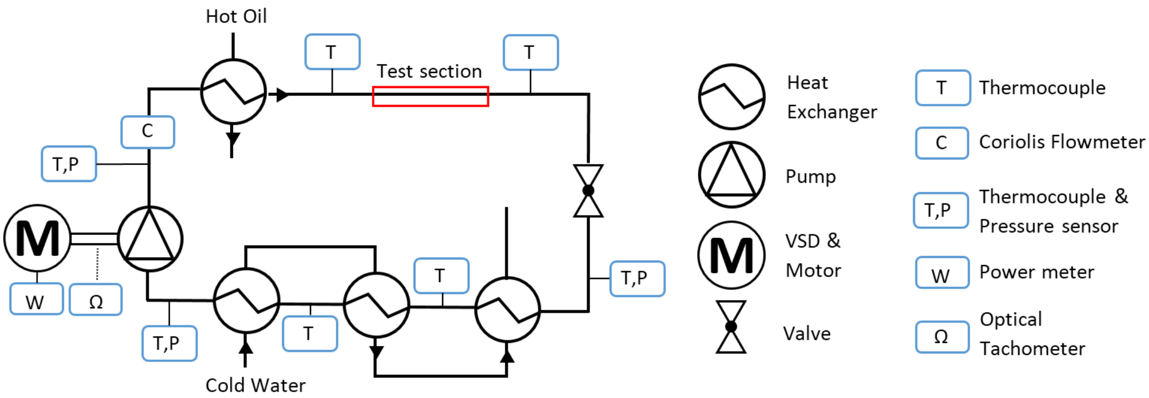

Figure 1: Scheme of the test bench

2.1 Test Bench

The pumping system is composed by a diaphragm pump (Wanner Hydra-Cell, model G03X), using a triplex single-acting reciprocating positive displacement technology. This technology is often used in small supercritical ORC because of its tightness and high efficiency at high pressure, low flow rate. And, a three-phase induction motor (Leroy-Sommer, model LS90L 1,8kW) integrating a Variable Speed Drive (VSD) (Leroy-Sommer, model Varmeca 32). The frequency can vary from 10 to 50 Hz, corresponding to a shaft rotational speed from 300 to 1500 revolutions per minute (rpm). At nominal speed (1500 rpm), the volume flow is around 0,58 m^3/h and the maximum outlet pressure is 70 bar. The pump is located at the bottom of the bench after all condensers to increase the NPSH. The fluid is evaporate and expanded through a valve that control the pressure differential at the pump ends. The electrical consumption is measured by a power quality clamp meter. The mass flow rate is measured by a Coriolis flowmeter. The shaft rotational speed is measured by an optical tachometer. Measurement accuracy are shown in Table 1.

2.2 Test Description

In order to characterize the pump, different kinds of tests are done. Since there is no torque meter between the motor and the pump, uncoupled motor tests are done to characterize the motor and VSD. Experimental data cover the full speed range, with 52 points. Unloaded pump test are done to estimate the unloaded volume flow ($\dot{V}_0$), valves are open to reduce the pressure differential at the pump ends (ΔP), 48 points cover the full speed range. For pump on load, total of 87 experimental points are achieved, covering a ΔP range from 0 to 35 bar at five different speed shaft (350 to 650 rpm). For each point, measurement are averaged during 1-2 minutes, to smooth variations. NPSH is kept as high as possible to reduce its impact on the volumetric efficiency (Miller, 1988).

Table 1 : Measuring range and accuracy

Variable	**Range**	**Uncertainty**
Supply pressure	0-17 bar	± 0,3 bar
Exhaust pressure	0-50 bar	± 0,1 bar
Temperature	0-120 °C	± 0,5 °C
Shaft rotational speed	0-1500 rpm	± 1 rpm
Electrical power	0-700W	± 20 W
Mass flow rate	0-0,1 kg/s	± 5.10^{-4} kg/s

3. DATA REDUCTION

3.1 System Energetic Model

An energetic model of the pumping system is proposed in Figure 2 to identify losses. $\dot{W}_{el}$ is the measured electrical consumption, $\dot{W}_{mech}$ is the mechanical shaft power, $\dot{Q}_{los}$ are powers dissipated by different components in the ambient environment. Fluid pumping is assumed to be fast enough to consider no heat transfer between the pump and the fluid. $\dot{W}_{flu,pp}$ the power transferred by the pump to the fluid is made of $\dot{W}_{hyd} = \int v.dP$ the hydraulic power (ie. useful) and internal frictions which are represented by a fictive heat power $\dot{Q}_{los,flu}$. Different efficiencies are defined from these power: the global efficiency of the pumping system $\eta_{global} = \dot{W}_{hyd}/\dot{W}_{el}$, the pump efficiency $\eta_{pump} = \dot{W}_{hyd}/\dot{W}_{mech}$ and the isentropic efficiency of the pump $\eta_{is} = \dot{W}_{hyd}/\dot{W}_{flu,pp}$.

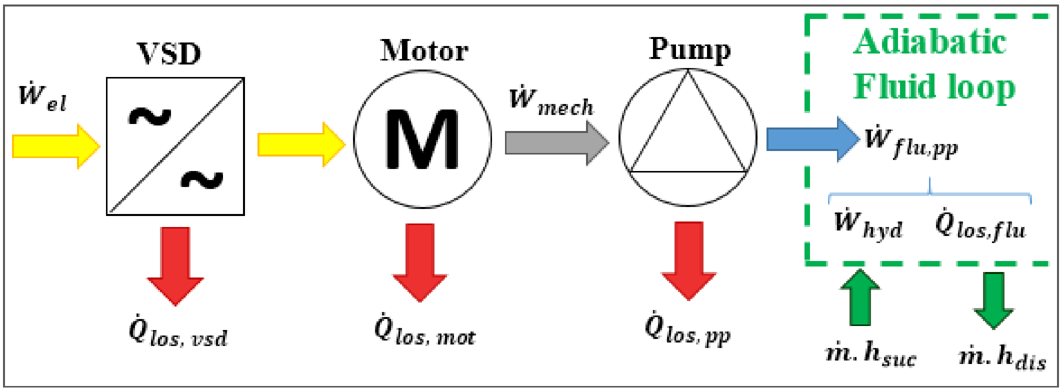

Figure 2: Energetic conceptual scheme of the pumping system

3.2 Motor and VSD Losses

Motor and VSD dissipated power should be estimated to get the mechanical power. Assumptions are made based on the literature review. De Almeida *et al.* (2014) and IEC 60034-31 explained that losses in VSD is a sum of constant loss and loss proportional to the output power. Kari (2009) performed tests and showed that in modern VSDs, losses increase with speed and torque. At low torque, losses are nearly constant and independent of the rotational speed. In tests performed for this study, motor and VSD operate under 50 % of the nominal torque. It is assumed that VSD losses ($\dot{Q}_{los,vsd}$) are constant, as did Deprez *et al.* (2010) for its VSD and motor losses approximation.

Induction motors have been more widely studied and normalized, even under variable speed and load. The IEC 60034-31 provide a part load efficiency formula based on manufacturer motor data. In this formula, motor losses are a linear function of $\dot{W}_{mech}^2$. Li *et al.* (2015) improved it with a new correlation for motor efficiency drive by a VSD, assuming the voltage is proportional to the frequency at the VSD output. From this correlation and assuming a constant power factor over the test, motor losses are expressed as: $\dot{Q}_{los,mot} = C_2.\dot{W}_{mech}^2 + C_3.\Omega^2$ with C_2 and C_3 constant parameters function of motor design. Figure 3 shows estimated losses for the motor used in this study, with both correlations. Correlations show small differences at nominal speed, correlation developed by Li is used for motor losses estimation. Therefore, the shaft power is estimated with one empirical constant (C_1) for VSD losses. $\dot{W}_{mot,n}$; $\eta_{mot,n}$; Ω_n are respectively the nominal motor power, the efficiency and the rotational speed, provided by the manufacturer. $\dot{W}_{el}$ and $\dot{\Omega}$ are measured parameters. The quadratic equation (1) is solved to find $\dot{W}_{mech}$.

$$\dot{W}_{mech} = \dot{W}_{el} - \dot{Q}_{los,vsd} - \dot{Q}_{los,mot} = \dot{W}_{el} - C_1 - \left[\left(\frac{1}{\eta_{mot,n}} - 1\right)\dot{W}_{mot,n}\left(0{,}7\,\frac{\dot{W}_{mech}^2}{\dot{W}_{mot,n}^2} + 0{,}3\,\frac{\dot{\Omega}^2}{\dot{\Omega}_n^2}\right)\right] \quad (1)$$

From uncoupled motor tests, assuming $\dot{W}_{mech} = 0$, experimental value of C_1 is find to be *240W*.

3.3 Pump Data

Volume flow rate is estimated from the mass flow rate and the fluid density using pressure and temperature at the pump outlet. Density, as other fluid properties, are computed with R-134a property equations provided by Tillner-Roth and Baehr (1994) used on EES. $\dot{W}_{flu,pp} = \dot{m}_{flu}.\Delta h_{pp}$ and enthalpy is computed from pressure and temperature. Hydraulic power is define as: $\dot{W}_{hyd}\ [W] = \dot{V}\ [m^3/s].\Delta P\ [Pa]$. Therefore, $\dot{Q}_{los,pp}$ and $\dot{Q}_{los,flu}$ are estimated. Volumetric efficiency is the ratio between the real volume flow ($\dot{V}$) and the theoretical flow, product of displaced volume by rotational speed ($\dot{V}_{th} = V_{disp}.\dot{\Omega}$). When the pump runs unloaded ($\Delta P = 0$), η_{vol} is near 100%. Therefore, manufacturer theoretical flow is compared with experimental no load flow ($\dot{V}_0$). Manufacturer displaced volume (V_{disp}) is estimated at 6,84 cm^3, experimental at 7,15 cm^3. Since the same method is used to estimate the volume flow on load and unloaded, experimental no load flow is taken to compute the volumetric efficiency: $\eta_{vol} = \dot{V}/\dot{V}_0$.

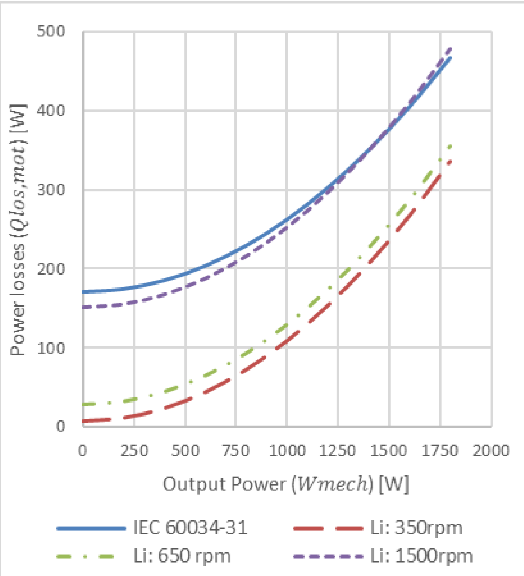

Figure 3: Motor losses function of load

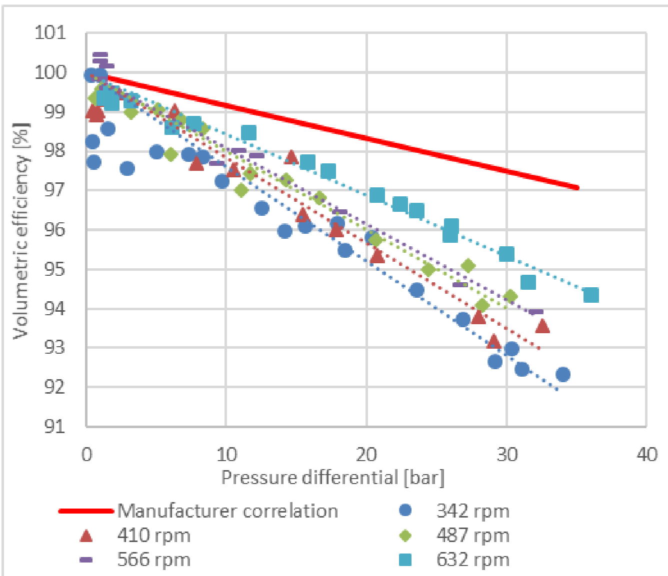

Figure 4: Effect of ΔP on volumetric efficiency for different mean rotational speed

4. RESULTS & ANALYSIS

4.1 Volumetric Efficiency

On load tests are performed at constant speed reference. Since an induction motor is used, slip increases between the speed reference and the real shaft speed when load increase. Therefore, the rotational speed should be measured at every step to compute corresponding no load flow and volumetric efficiency. As shown in Figure 4 volumetric efficiency if found to be dependent of the pressure differential and rotational speed while in theory, manufacturer data shown it is only proportional to the ΔP. Manufacturer and experimental result should be compared with caution since manufacturer data are mainly computed for cold water.

Literature shows different factors affecting the volumetric efficiency. As previously noted, NPSH affects the volumetric efficiency (Miller, 1988). For reciprocating pump, the NPSHr is defined by ANSI/HI 6.1-6.5 and 6.6 as a reduction of 3 % in the volumetric efficiency compared to the max efficiency, at the same speed and pressure differential. Therefore, sub-cooling is essential to keep a good volumetric efficiency. Here, NPSH impact is neglected. Reciprocating pumps use valves, Miller (1995), Singh and Madavan (1987) and Johnston (1991) mentioned continuous valve leakage under high pressure and backflow when piston changes direction due to delays in the valves closing. If the closing delays is assumed to be inversely proportional to the rotational speed and since the number of cycle is proportional to the rotational speed, the average backflow time is considered constant. Therefore, backflow and continuous leakage are approximated by a continuous leakage flow rate using the equation proposed by De Chargeres and Rey (2009): $\dot{V}_{leak} = A.\Delta P/\mu$ with A an empirical geometric coefficient.

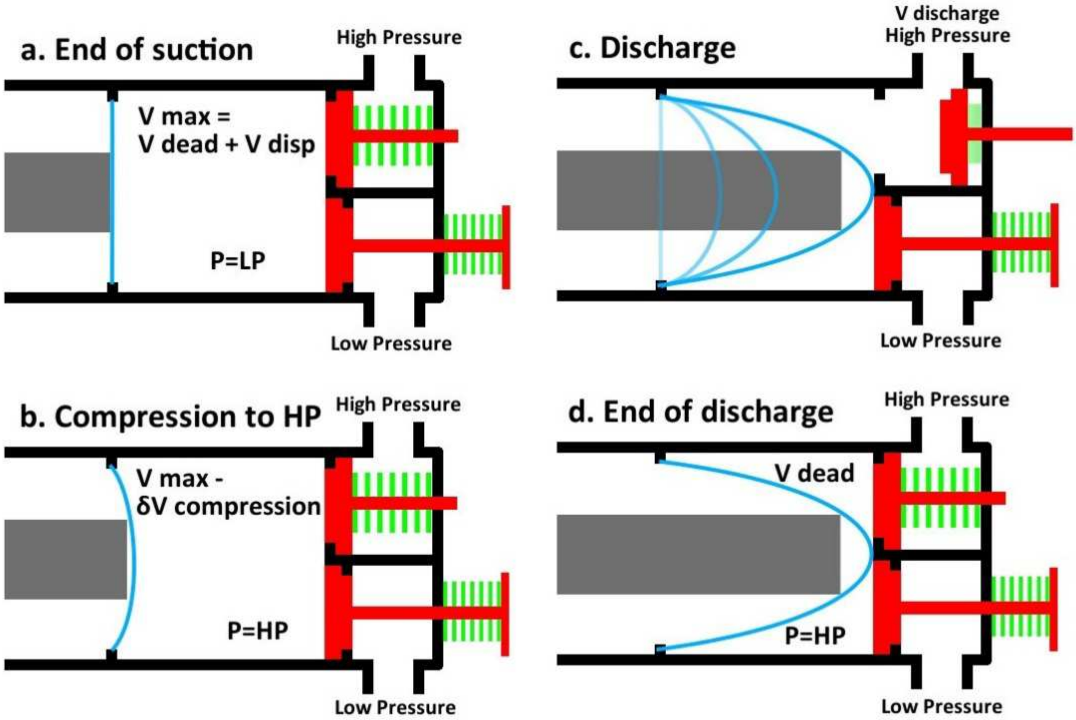

Figure 3: Reciprocating pump discharge process

Fluid compressibility is the third and most important factor. This factor creates a likelihood of confusion: the volumetric efficiency could be defined using the suction (Tackett *et al.*, 2008) or the discharge volume flow rate (Miller, 1995). Since outlet conditions are used to compute the volume flow, the second formulation is used. Figure 5 presents steps of the discharge process. Isothermal compressibility factor $\beta_T = -\frac{1}{V}.\left(\frac{\delta V}{\delta P}\right)_T$ is introduced to write the volume discharge per stroke:

$$V_{dis} = (V_{max} - \Delta V_{compression}) - V_{dead} = V_{disp} - \Delta P.\beta_T.(V_{disp} + V_{dead}) \tag{2}$$

Adding valve leakage, discharge flow and volumetric efficiency equations are:

$$\dot{V}_{dis} = \dot{\Omega}.V_{disp}.\left(1 - \Delta P.\beta_T.\left(1 + \frac{V_{dead}}{V_{disp}}\right)\right) - A.\frac{\Delta P}{\mu} \tag{3}$$

$$\eta_{vol} = \frac{\dot{V}_{dis}}{\dot{\Omega}.V_{disp}} = 1 - \Delta P.\beta_T\left(1 + \frac{V_{dead}}{V_{disp}}\right) - \frac{A.\Delta P}{\mu.V_{disp}.\dot{\Omega}} \tag{4}$$

$$= 1 - \left(\frac{C_4}{\dot{\Omega}} + C_5\right).\Delta P \quad \text{with } C_4 = \frac{A}{\mu.V_{disp}} \quad \text{and } C_5 = \beta_T.\left(1 + \frac{V_{dead}}{V_{disp}}\right) \tag{5}$$

Slope coefficients of Figure 4 are reported in Figure 6 corresponding to $(a/\Omega + b)$ coefficient. V_{disp} is known from 3.3, μ and β_T are fluid properties computed from outlet conditions. Therefore, geometrical leakage coefficient is estimated $A \cong 1{,}3.10^{-10}\,cm^3$ and the dead volume $V_{dead} \cong 5{,}5\,cm^3$. Uncertainties on those values are high since there are only five data points used. Data at nominal speed will give more confidence in those results. However, manufacturer slope is constant, which could be explained if valve leakages were neglected ($C_4=0$), and leads to a single coefficient $C_5=0{,}000835\ bar^{-1}$, close to the experimental one ($C_5=0{,}000837$).

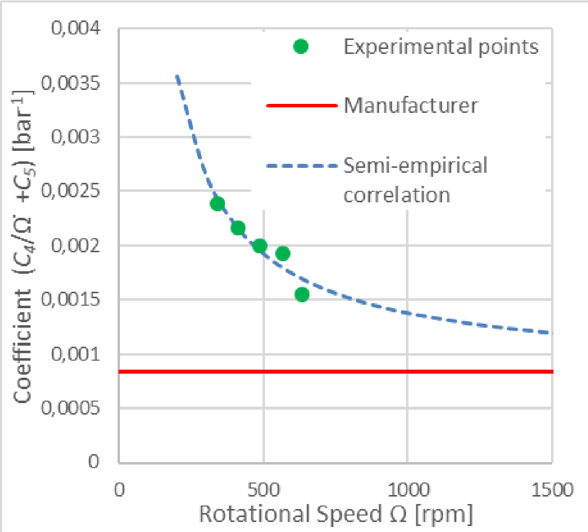

Figure 6: Volumetric efficiency slope coefficient

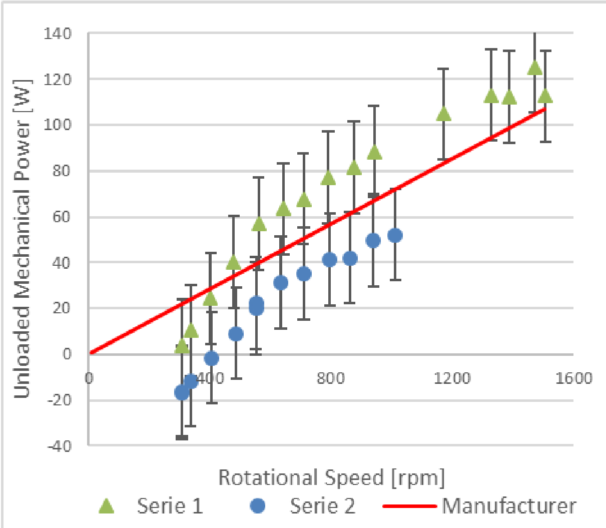

Figure 7: Unloaded mechanical power

4.2 Power & Pump Efficiency

Manufacturer proposes an equation to estimate the required power:

$$\dot{W}_{mech} = C_6.\dot{\Omega} + C_7.\dot{W}_{hyd} \tag{6}$$

The first term corresponds to friction losses, the second to pumping work efficiency. Manufacturer coefficient values are compared with experimental data. Coefficient C_6 is estimated from unloaded tests, the hydraulic power is neglected. For more accuracy, VSD and motor losses are not computed from Equation (1) to estimate $\dot{W}_{mech}$. Instead, experimental losses from uncoupled tests is used. In addition, the hydraulic power, even low, is subtracted (assuming $C_7=1$). Figure 7 shows two series of test and the linear interpolation, C_6 is estimated at *0,0723 W/rpm* with the same order of magnitude as the manufacturer value: *0,0711 W/rpm*. From on load tests, coefficient C_7 is estimated at *1,212* (manufacturer: *1,174*). Mechanical power computed from motor & VSD model (Equation 1 with experimental $\dot{W}_{elec}$) and pump model (Equation 6 with experimental $\dot{W}_{hyd}$) are compared in Figure 8.

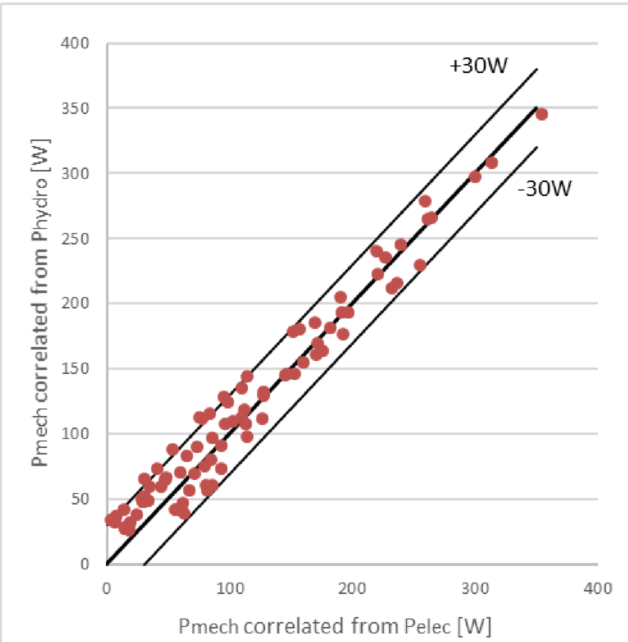

Figure 8: Correlated Mechanical Power: Pump model (equation 6) *vs* Motor model (equation 1)

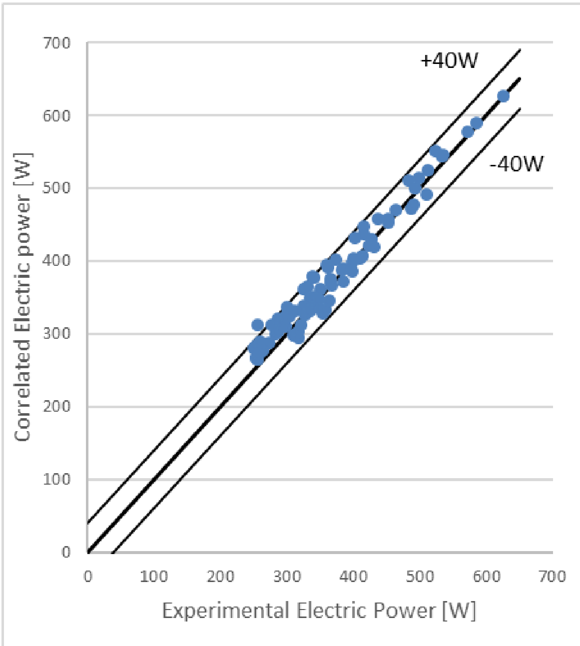

Figure 9: Experimental vs Correlated Electric Power

From Equation (6), pump efficiency becomes $\eta_{pump} = \dot{W}_{hyd}/(C_6.\dot{\Omega} + C_7.\dot{W}_{hyd})$ Miller (1995) and Tackett (2008) have the same kind of pump efficiency dependence with the load. The maximum pump efficiency is directly revealed: $\eta_{pump,max} = 1/C_7 = 82{,}5\%$. Power consumption $\dot{W}_{el}$ is estimated from $\dot{W}_{hyd}$ and $\dot{\Omega}$ using Equation (1) and (6), experimental and correlated values are compared in Figure 9.

Enthalpies are not known with enough accuracies to provide accurate $\dot{W}_{flu,pp}$ and therefore isentropic efficiencies values. A solution should be to use more accurate temperature sensors or use a calorimeter to estimate $\dot{Q}_{los,pp}$. However, the isentropic efficiencies mean trend seems similar to the pump efficiency trend. If $\dot{Q}_{los,pp}$ is assumed negligible, then, as a first approximation $\eta_{is} \cong \eta_{pump}$.

4.2 Model Overview

Table 2 summarize the main equation useful for the pumping system modelling. The first equation provide a relation between the volume flow (or the volumetric efficiency), the shaft rotational speed and the pressure drop. It could be used for flow control purpose or volume flow rate estimation. The second equation provide a relation between the pump mechanical shaft power, the rotational speed, the pressure drop and the flow rate. The flow rate could be compute from the first equation. This equation is use for pump losses and efficiency. The third equation provide a relation between the electric consumption, the rotational speed and the motor shaft power. When each equation are combined, it provide the net electric power request for a given pressure drop and rotational speed (or flow rate). This is useful for modelling or design purpose.

Table 2 : Models equations and parameters overview

Volume Flow Rate	$\dot{V}_{dis} = \dot{\Omega}.V_{disp}\left[1 - \left(\frac{A}{\dot{\Omega}.\mu.V_{disp}} + \beta_T.\left(1 + \frac{V_{dead}}{V_{disp}}\right)\right).\Delta P\right]$			
Input parameters	$\dot{\Omega}$	rpm	Rotational speed	
	ΔP	bar	Pressure differential	
Model coefficients	V_{disp}	m^3	Displaced volume	*Experimental*: Unloaded pump test
	A	m^3	Leakage coefficient	*Experimental*: On-load pump test
	V_{dead}	m^3	Dead volume	
Fluid properties	μ	Pa.s	Dynamic viscosity	Computed from outlet pressure & temperature
	β_T	Pa^{-1}	Isothermal compressibility	
Pump power	$\dot{W}_{mech} = C_6.\dot{\Omega} + C_7.\dot{W}_{hyd} = C_6.\dot{\Omega} + C_7.\dot{V}_{dis}.\Delta P$			
Input parameters	$\dot{\Omega}$	rpm	Rotational speed	
	ΔP	Pa	Pressure differential	
	$\dot{V}_{dis}$	m^3/s	Volumetric flow	
Model coefficients	C_6	W/rpm	Friction coefficient	*Experimental*: On-load pump test
	C_7	-	Efficiency coefficient	
VSD & Motor power	$\dot{W}_{el} = C_1 + \dot{W}_{mech} + C_2.\dot{W}_{mech}^2 + C_3.\dot{\Omega}^2$			
Input parameters	$\dot{\Omega}$	rpm	Rotational speed	
	$\dot{W}_{mech}$	W	Mechanical power	
Model coefficients	C_1	W/rpm	VSD losses coefficient	*Experimental*: Uncoupled motor test
	C_2	W^{-1}	Part-load coefficient	*Motor data :* $C_2 = 0{,}7.\frac{(1/\eta_{mot,n} - 1)}{\dot{W}_{mot,n}}$
	C_3	W/rpm²	Motor friction coefficient	*Motor data :* $C_3 = 0{,}3.\dot{W}_{mot,n}.\frac{(1/\eta_{mot,n} - 1)}{\dot{\Omega}_n^2}$

6. CONCLUSIONS

An energetic analysis of a pumping system for ORC is proposed. For each component, a semi-empirical power model based on literature and experimental analysis is presented. This model could be used for the design or simulation of a reciprocating pump integrated into an Organic Rankine cycle, at part and full load. The volumetric efficiency equation could be used for simulation, process control or flow rate estimation if no flowmeter is available. Clarification of the different efficiencies useful for ORC design or simulation is proposed. The method and model deserve a deeper investigation for validation, as torque measurement between motor and pump or VSD electric power output. Measurement are in progress on a bigger pump for comparison and scale-up. .Experimental analysis shows that reciprocating pump can achieve good efficiency at high pressure (more than 80%), but falls when the pressure decrease. Pump driver should be carefully chosen and designed as well as the pump. Oversize leads to lower efficiency, especially when the process runs often at part-load operation. The electric motor should be chosen according to the process nominal power and not the pump maximum power, avoiding a motor oversizing due to pump oversize. It should also be noted that new legislation on motor minimal efficiency are implemented in most countries.

NOMENCLATURE

h	specific enthalpy	(J/kg)	$\dot{W}$	power	(W)
$\dot{m}$	mass flow rate	(kg/s)	β_T	isothermal compressibility	(Pa^{-1})
P	pressure	(bar)	Δ	difference	(-)
$\dot{Q}$	heat power	(W)	η	efficiency	(-)
V	volume	(m^3)	μ	dynamic viscosity	(Pa.s)
$\dot{V}$	volume flow rate	(m^3/h)	$\dot{\Omega}$	rotational speed	(rpm)

Subscript

0	unloaded	mech	mechanical
dis	discharge	mot	motor
disp	displaced	n	nominal
el	electrical	pp	pump
flu	fluid	suc	suction
hyd	hydraulic	th	theory
is	isentropic	vol	volumetric
los	losses	vsd	variable speed drive

REFERENCES

Astolfi, M., Romano, M.C., Bombarda, P., Macchi, E., 2014. Binary ORC (Organic Rankine Cycles) power plants for the exploitation of medium–low temperature geothermal sources – Part B: Techno-economic optimization. *Energy*, vol. 66: p. 435–446

Bao, J., Zhao, L., 2013. A review of working fluid and expander selections for organic Rankine cycle. *Renewable and Sustainable Energy Reviews*, vol. 24: p. 325–342

De Almeida, A., Falkner, H., Fong, J., Jugdoyal, K., 2014. EuP lot 30 - Electric motors and drives (Final Report). for European Commission: 209p.

De Chargeres, B., Rey, R., 2009. Pompes volumétriques pour liquides, *Techniques de l'Ingénieur*.

Deprez, W., Lemmens, J., Vanhooydonck, D., Symens, W., Stockman, K., Dereyne, S., Driesen, J., 2010. Iso efficiency contours as a concept to characterize variable speed drive efficiency. *10th International Conference on Electrical Machines*, Rome.

Maraver, D., Royo, J., Lemort, V., Quoilin, S., 2014. Systematic optimization of subcritical and transcritical organic Rankine cycles (ORCs) constrained by technical parameters in multiple applications. *Applied Energy*, vol. 117: p. 11–29.

Miao, Z., Xu, J., Yang, X., Zou, J., 2015. Operation and performance of a low temperature organic Rankine cycle. *Applied Thermal Engineering*, vol. 75: p. 1065–1075

Miller, J.E., 1988. Characteristic of the reciprocating pump. *Proc. of the 5th International Pump Users Symposium*, Houston.

Miller, J.E., 1995. *The Reciprocating Pump Theory, Design, And Use*, Krieger Publishing Co: 484 p.

Johnston, D.N., 1991. Numerical modelling of reciprocating pumps with self-acting valves. *Proceedings of the Institution of Mechanical Engineers, Part I: Journal of Systems and Control Engineering*, vol. 205: p. 87–96.

Kari, R., 2009. AC Drive comes with losses - Technical Description. ABB.

Li, Y., Liu, M., Lau, J., Zhang, B., 2015. A novel method to determine the motor efficiency under variable speed operations and partial load conditions. *Applied Energy*, vol. 144: p. 234–240

Lippke, F., 1995. Simulation of the part load behavior of a 30 MWe SEGS plant. Sandia National Laboratories

Quoilin, S., Aumann, R., Grill, A., Schuster, A., Lemort, V., Spliethoff, H., 2011. Dynamic modeling and optimal control strategy of waste heat recovery Organic Rankine Cycles. *Applied Energy*, vol. 88: p. 2183–2190

Quoilin, S., Broek, M.V.D., Declaye, S., Dewallef, P., Lemort, V., 2013. Techno-economic survey of organic rankine cycle (ORC) systems. *Renewable and Sustainable Energy Reviews*, vol. 22: p. 168–186

Schuster, A., Karellas, S., Aumann, R., 2010. Efficiency optimization potential in supercritical Organic Rankine Cycles. *Energy*, vol. 35: p. 1033–1039

Shu, G., Liu, L., Tian, H., Wei, H., Xu, X., 2013. Performance comparison and working fluid analysis of subcritical and transcritical dual-loop organic Rankine cycle (DORC) used in engine waste heat recovery. *Energy Conversion and Management*, vol. 74: p. 35–43.Astolfi, M., Romano, M.C.,

Singh, P.J., Madavan, N.K., 1987. Complete Analysis and Simulation of Reciprocating Pumps Including System Piping. *Proc. of the 4th International Pump Users Symposium*, Houston, p. 53–73.

Tackett, H.H., Cripe, J.A., Dyson, G., 2008. Positive Displacement Reciprocating Pump Fundamentals - Power and Direct Acting Types. *Proc. of the 24th International Pump Users Symposium*.

Tillner-Roth, R., Baehr, H.D., 1994. An International Standard Formulation for the Thermodynamic Properties of 1,1,1,2-Tetrafluoroethane (HFC-134a) for Temperatures from 170 K to 455 K and Pressures up to 70 MPa. *Journal of Physical and Chemical Reference Data*, vol. 23: p. 657.

Toffolo, A., Lazzaretto, A., Manente, G., Paci, M., 2014. A multi-criteria approach for the optimal selection of working fluid and design parameters in Organic Rankine Cycle systems. *Applied Energy*, vol. 121: p. 219–232.

Vetter, G., 2006. *Rotierende Verdrängerpumpen für die Prozesstechnik*, Vulkan-Verlag GmbH. 337 p.

ANSI/HI 6.1-6.5, 2000. Reciprocating Power Pumps for Nomenclature, Definitions, Application and Operation. American National Standards Institute.

ANSI/HI 6.6, 2000. Reciprocating Pump Tests. American National Standards Institute.

IEC 60034-31, 2010. Guide for the selection and application of energy efficient motors including variable-speed applications. International Electrotechnical Commission.

ACKNOWLEDGEMENT

This work was supported by the French Environment and Energy Management Agency (ADEME) and the Atomic Energy Commission (CEA)